Proceedings of the Canadian Society for Mechanical Engineering International Congress 2022
CSME Congress 2022
June 5-8, 2022, Edmonton, AB, Canada

Design and Development of a Novel Tensile Testing Apparatus for Time-Resolved Betatron X-Ray Tomographic Imaging

Alvaro R. Arce-Borkent[1], Tait Richards[2], Vigneshvar Senthilkumaran[2], Nicholas F. Beier[2], Le Zhou[3], John A. Moore[3], K. Steven Knudsen[2], Amina E. Hussein[2], Michael G. Lipsett[1*]
[1]Department of Mechanical Engineering, University of Alberta, Canada
[2]Department of Electrical and Computer Engineering, University of Alberta, Canada
[3]Department of Mechanical Engineering, Marquette University, USA

Abstract

High-resolution imaging of deformation processes in materials under load requires controllable and stable loading conditions and the ability to vary sample orientation relative to the imaging source. A novel tensile testing apparatus has been designed, developed, and characterized for time-resolved imaging of defect formation and evolution in additively manufactured (AM) using compact laser-driven betatron x-ray sources. The system allows controllable tensile loads to be applied to small diameter samples and enables stepwise rotation for tomographic x-ray imaging. Several improvements have been made to the original design to ensure consistent testing conditions and imaging quality[1].

Keywords-component; Additive Manufacturing, plasma-based accelerators, x-ray imaging, experimental apparatus, materials testing.

I. INTRODUCTION

Betatron x-rays produced by a laser wakefield accelerator (LWFA) [1] are used for various applications in medicine, engineering, and science [2-8]. Recent work has demonstrated that these laser-driven sources can provide an alternative to conventional synchrotron beamlines [8] and x-ray microcomputed tomography [7] for high-resolution imaging of complex structures, enabling rapid data acquisition using a system that can be housed in a standard-size laboratory. The compact nature of these novel light sources requires the development of similarly compact equipment. For time-resolved betatron x-ray imaging of defect formation and evolution in additively manufactured (AM) alloys [8], small diameter (~mm) samples are placed under different loads and driven to fracture. For tomographic imaging, rotation of these samples is required. Pursuit of this experimental work requires the development of a compact, full rotation-capable tensile test frame suitable for operation in a high-power laser lab.

The betatron x-ray tensile tester is a co-op student-designed device in support of research into the porosity characterization of AM alloys undergoing tensile stress. Requirements for the tester include: uniaxial tension of up to 5 kN to a few-millimeter diameter rod (made from additively manufactured AlSi10Mg) that may vary in length from 10 to 150 mm, rotation of the sample while under tension to at least 180 degrees in 0.5-degree steps, providing up to 360 incident beam profile possibilities with a clear line of sight without applying any cyclic loading, compatibility with standard optical tables, simple sample mounting and replacement, and clear access for instruments and accessories.

This paper describes the process for designing a compact tensile tester suitable for use in betatron x-ray imaging experiments, while exploring various mechanism concepts and control alternatives.

II. TENSILE FRAME CONCEPTS

The initial concept, inspired by current, modern tensile testing systems such as Instron's Universal testers [9], was a tower comprising a single support column, sample holders, and an axial force generator, with the specimen secured in an upright position. The entire device would rotate about the sample long (vertical) axis with the line-of-sight rotation extent limited by the width of the support column. This approach suffered from poor access to the sample and limited imaging views.

To eliminate the support column, a modified design inspired by Bruker 3D x-ray microscopes [10] was investigated. The concept of using an x-ray transparent cylinder to replace the column is shown in Figure 1. However, several limitations of this design were noted. In particular, the sample supports and

This work was supported by the US Department of Energy Office of Fusion Energy Sciences LaserNetUS (proposal K136): the LaserNetUS initiative at the Advanced Laser Light Source at the Institut National de la Recherche Scientifique, Lawrence Livermore National Laboratory under Subcontract B643845 and the Natural Sciences and Engineering Research Council of Canada (NSERC grant no. RGPIN-2021-04373). The University of Alberta Engineering Co-op Office provided work term support for A. Arce-Borkent, R. Tait, and J. Kaminsky.

*Corresponding author: mlipsett@ualberta.ca

force actuator size would mean the diameter of the support cylinder would be relatively large, limiting access to the sample during imaging. Changing samples would be tedious because the top support and cylinder itself would have to be removed. These and other factors motivated a new approach.

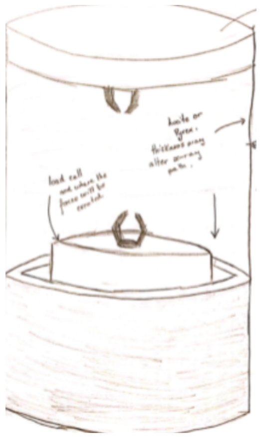

Figure 1. Early conceptual sketch of a vertical design.

The final design is influenced by commercial computer numerical control (CNC) mini-lathes, such as Sherline products [11], and addresses the previous design shortcomings. The key innovation is to incorporate the axial force actuator and sensor into the CNC stepped rotational mechanisms with all load transmitted through an offset structure, as is the case in a conventional lathe. This feature enables 360 degrees of imaging access without intervening support structures. As shown in Figure 2, the narrow long-axis structure means that test and measurement instruments on an optical table can be positioned close to samples. A linear actuator attached to a stepped rotary table provides the axial force while a load cell attached to a second stepped rotary table measures the force. The actuator's horizontal placement requires a support saddle, which was machined from Teflon. The assemblies are mounted on a flat support plate that can be readily attached to a standard optical table. Figure 3 shows the final built tensile tester with the replacement of the headstock by a rotary table.

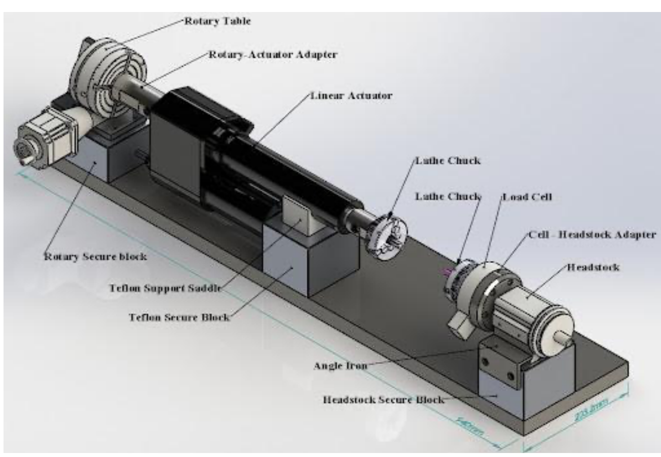

Figure 2. CAD rendering of the final design.

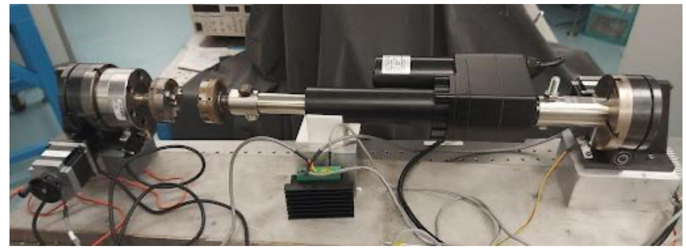

Figure 3. Tensile tester as built with second rotary table.

III. CONTROL AND SENSING DESIGN

A. Hardware and Interfaces

The control and sensing design process began after the initial mechanical design was complete. The first step was choosing viable electronic hardware and software components to bring the machine into a functional state. We decided to use a Raspberry Pi 3B for the microcontroller as it would interface with the hardware and provide a web interface to control the machine. We also used an OpenScale [12] that provides a serial interface to the load cell. A TB6600 stepper motor driver drives both rotary tables. The primary software component chosen was Node-RED [13] as it supports a web interface served from the Raspberry Pi, accepts the required inputs, and provides the required outputs, either through serial or GPIO pins. Custom C programs (based on the `pigpio` library) interface with the stepper driver. C was chosen as Node-RED is unable to produce the precise timing required to operate the stepper driver adequately. These choices are illustrated in Figure 4.

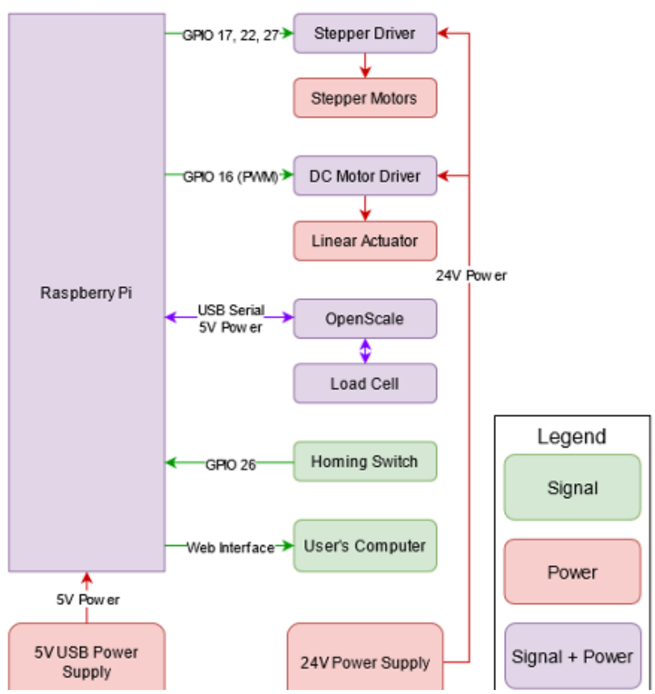

Figure 4. Sensing and control functional block diagram.

The Raspberry Pi is connected to the other hardware components in three different ways, as shown in Figure 4. The rotary table stepper motor drivers are connected using GPIO 17 for the step signal, GPIO 22 for the direction signal, and GPIO 27 for the enable signal. The DC actuator motor driver is controlled using pulse-width modulation (PWM) over GPIO 20. The homing switch is read from GPIO 26. The motor drivers are also hooked up to the 24 V power supply. The OpenScale is connected to the Raspberry Pi on the serial port /dev/ttyUSB0 using the 8n1 9600 baud protocol. The user's computer is connected through the Raspberry Pi's web interface.

B. Software

The other major part of the control and sensing design process was the software control of the machine. The idea was for the machine to be controllable from another room as it would be placed in the path of an x-ray beam. This was achieved using a Node-RED web interface that allowed the rotary motion, tension control, and zeroing / calibration of the rotational axis and load cell. Although Node-RED could directly control the GPIO pins, it could not do so with enough precision to properly control the motor drivers. Three C programs were written that interface with the motor drivers. This was done using the `pigpio` library [14], which allowed for the creation of waveforms and PWM signals that could be sent to the GPIO pins. The interconnection between the software and hardware components is detailed in the block diagram of Figure 5.

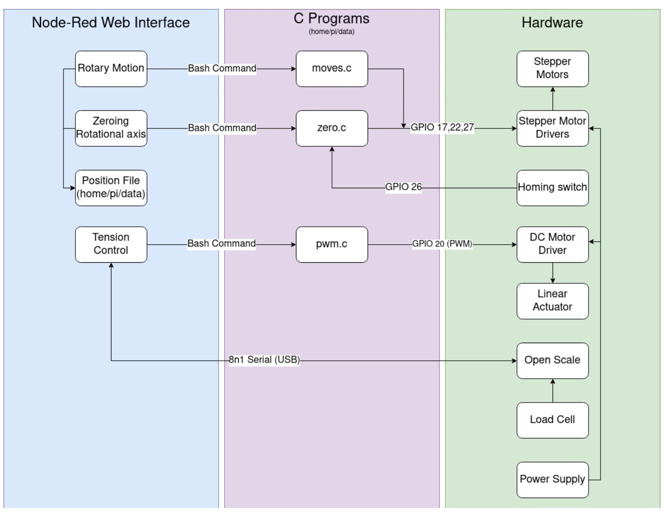

Figure 5. Hardware and software interconnection.

The three C programs can be seen in the above diagram, and each had a specific purpose. The first program, `moves.c`, rotates the machine a specific amount of steps in either direction at a ramping speed. The second program, `zero.c`, rotates the machine to the zero position specified by the homing switch. The third program, `pwm.c`, provides a PWM signal to the DC motor driver that controls the speed of the actuator and changes the tension on the sample.

The software implemented multiple control methods to precisely rotate the sample to any position without applying potentially damaging torque to the thin sample. Provisions to prevent damage to the system from cables wrapping as the sample rotates, over-rotating the frame or zeroing the machine in a dangerous position are also implemented.

The load cell can be read and calibrated quickly through the serial interface provided by the OpenScale. Initially, control of the actuator was problematic. The initial plan was to set a tension value and to have the system automatically move the actuator to achieve the desired tension. This proved unwieldy as the actuator could move quite quickly and forcefully, overshooting the desired tension and prematurely breaking the sample. When the speed was reduced by changing the PWM parameters and thereby lowering the applied analog voltage, the actuator would not apply the required force to suitably break the sample.

Furthermore, the load cell would only report the tension value at a maximum of 10 samples per second, and the signal was rather noisy at the highest rate. This was addressed by allowing the user to move the actuator in multiple ways: automatic control, stepped manual mode, and continuous manual mode. The stepped manual mode provided the most accurate sample tension. Improved automatic tension control could have been achieved using an alternative feedback control scheme and signal processing for noise reduction. This was not implemented as the tension reporting rate proved inadequate. Most tensile testing machines can operate based on displacement (total strain on the sample) rather than force controlled. The linear actuator has a potentiometer that measures position data; however, its precision was far from the sub 1 mm required for the application. An acceptable compromise was to modify the apparatus with a stepper motor-driven actuator that could move precisely and accurately, allowing for more conventional position-based control. This actuator was not implemented until after a preliminary run of experiments.

Another necessary feature of the system was the ability to log displacement and tensile force data locally on the Raspberry Pi as part of system characterization. The system was set up to record the rotational position, tension value, and timestamp into a file up to 10 times per second when logging was enabled.

IV. CHALLENGES AND SOLUTIONS

It was clear during commissioning and early trials that the standard lathe chucks would not be suitable for withstanding the axial load when tensioning the samples. An alternative fixture approach was considered with collets, but this was initially rejected due to a relative lack of versatility compared to the lathe chuck to handle larger-sized samples in future experiments. The actuator was modified to incorporate feedback control of a heavy-duty linear actuator providing over 8 kN of tensile strength, chosen for controllability and versatility in loading larger samples. The rotary table can rotate in 0.1-degree increments with 3600 increments without interpolation, which exceeded the minimum rotational requirement.

The systematic loading error of applying torque at only one end of the sample would violate the intended loading condition. To mitigate torque being applied through the sample, two approaches were considered to keep the angle of both ends the same: a mechanical drive mechanism and a second rotating stage with an electronic controller to match angular positioning. The second rotating stage was implemented.

An alignment issue was discovered during initial trials: the center of the stage with the linear actuator was prone to drifting from the center of the other end, which put an undesired bending moment into the sample. The saddle for the linear actuator was redesigned with a needle-bearing housing to improve concentricity, and other minor changes were made to improve assembly alignment of the assembly while reducing weight.

V. RESULTS AND FFUTURE WORK

A first iteration of the designed tensile test frame was deployed on experiments using the betatron x-ray beamline at the Advanced Laser Light Source [15] at the Institut national de la recherche scientifique in Varennes, Québec in September and November 2021 [16]. During these experiments, betatron x-ray generation and imaging capabilities up to 2.5 Hz operation were optimized for x-ray flux and experimental operation for high-throughput data collection. AlSi10Mg alloys were 3D printed by Vertex Manufacturing specifically to have large pores sizes to facilitate imaging of pore evolution. A sample with diameter 1 mm and 104 mm length was mounted between the chucks of the compact tensile test frame, as shown in Figure 6a). The betatron x-ray imaging was performed using an Andor iKon x-ray CCD camera with pixel size of 13 µm x 13 µm. at source to sample distance of 81 cm and sample to camera distance of 155 cm, yielding 2.9x magnification. An example betatron x-ray image of this sample shown in Figure 6b), where pores on the order of 10-80 µm are visualized. Enhanced requirements for the tensile test frame in terms of connectivity and alignment were also identified and addressed in subsequent updates to the design of the tensile test frame.

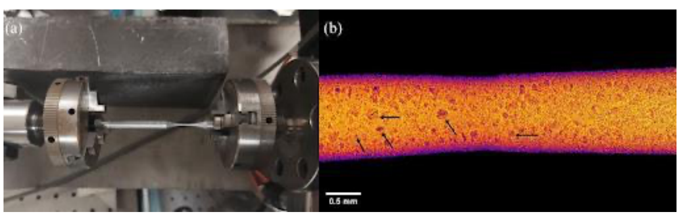

Figure 6. a) A sample mounted in the tensile tester. b) An example betatron x-ray image of the sample.

The aim of betatron imaging experiments is to compare the evolution of pores in AM AlSi10Mg alloys with different loading directions and triaxialities. For metals under tension, microscale pores (i.e., voids in the material) nucleate, grow, and coalesce to form larger pores and cracks that ultimately cause the failure of materials. However, this process is complex and not fully understood, even for traditionally manufactured materials [17]. Furthermore, AM materials are known to have directionally dependent properties due to the layer-by-layer approach to their manufacturing [18]. However, to date, there is little data on pore evolution in AM materials, let alone well time-resolved porosity data including effects of different build directions and at different triaxialities. Using ultrafast betatron x-ray imaging, we seek to obtain time-resolved porosity data on the effects of different build directions and triaxialities on porosity evolution in AM alloys. Porosity evolution curves are crucial to understanding the complex fracture mechanisms of advanced materials.

In upcoming experiments, x-ray tomography will be performed by placing the samples in a transmission geometry between the diverging x-ray beam and detector and rotating the sample through 90 degrees using the designed tensile test frame. The effect of loading direction and triaxiality on porosity evolution in AM AlSi10Mg will be investigated by applying increments of ~2kg on the sample using the tensile test frame presented in this paper, enabling investigation of pore dynamics at ~5 increments prior to material fracture. In practice, the data acquisition rate depends on the backing pressure of the ultrasonic gas jet driving the betatron x-ray source, the time required to rotate the sample (typically taking 1-2 seconds between each position), the CCD read time (typically 1 second), and the number of laser shots required for optimized imaging. With the optimized operation, a 90-degree tomographic scan of a single load position with one-degree steps could be performed on the order of 10 minutes, as compared to the order of hours for a micro-computed tomography device. This application of betatron x-ray sources to obtain high-throughput measurements of porosity dynamics in AM materials for the first time is an important proof-of-concept experiment for the further application of compact, laser-driven sources for materials characterization.

VI. CONCLUSION

In this paper, we have demonstrated the design and fabrication of a compact tensile testing apparatus suitable for use in compact betatron x-ray imaging experiments conducted in a high-power laser laboratory. The apparatus met requirements of delivering uniaxial tension up to 5 kN to 6-millimeter or smaller diameter rods while enabling up to 180 degrees of rotation at 0.5-degree increments with a clear line of sign for the x-ray beam. Further considerations such as compatibility with standard optical tables and ease of sample mounting and replacement were achieved.

A hardware-software interface for control and sensing of the apparatus was also developed in Node-RED, employing a Raspberry Pi 3D microcontroller and OpenScale for communication with and calibration of the load cell. Custom C programs were developed to interface with the stepper driver, enabling both displacement and force control of the tensile test system. Careful considerations to mitigate over-rotation of the frame, zeroing of the machine in a dangerous position, and excess torque applied to thin samples were taken in the design of this software.

The compact tensile testing apparatus was successfully deployed in preliminary experiments at the Advanced Laser Light Source in Varennes, QC, Canada in late 2021, demonstrating compatibility of the design with operation requirements in a high-power laser laboratory. Additively manufactured AlSi10Mg samples of 1 mm diameter and ~100 mm length were imaged using betatron x-rays with successful imaging of pores on the order of 10s of micrometers. The tensile testing apparatus will be deployed in upcoming experiments in 2022 to apply controlled tension to AM samples, enabling x-ray imaging of pore evolution dynamics leading up to material fracture.

This work aims to obtain critical data to form porosity evolution curves needed to validate detailed models of material degradation and explain the underlying mechanisms driving ductile fracture in AM alloys.

ACKNOWLEDGMENTS

We acknowledge J. Kaminsky, S. Meschian (Department of Mechanical Engineering, University of Alberta) and J. Stinehart and P. Shabaninezhad (Department of Mechanical Engineering, Marquette University), for their assistance in tensile test frame design. We also acknowledge Dr. S. Fourmaux (Institut National de la Recherche Scientifique– Énergie Matériaux et Télécommunications, Varennes, Québec, Canada) and the Advanced Laser Light Source experimental team for their contributions to experimental design and assistance with betatron x-ray imaging and Sean Dobson (Vertex Manufacturing/ University of Cincinnati) for assistance with 3D printing of AlMgSi alloys.

REFERENCES

[1] T. Tajima and J. M. Dawson, "Laser Electron Accelerator," Phys. Rev. Lett. Vol. 43,4, pages 267-270, 1979

[2] S.Kneip, C. McGuffey, J.L Martins, et al., "Bright spatially coherent synchrotron x-rays from a table-top source," Nature Physics, Vol. 6, pages 980-983, 2010

[3] J. Wenx, S. Schleede, K. Khrennikov, et al., "Quantitative x-ray phase-contrast microtomography from a compact laser-driven betatron source," Nature Communications Vol. 6, Article 7568, 2015

[4] J. M. Cole, J.C. Wood, N.C. Lopes, et al. "Laser-wakefield accelerators as hard x-ray sources for 3D medical imaging of human bone," Scientific reports, Vol. 5, page 1-7, 2015

[5] Felicie Albert and Alec G R Thomas, "Applications of laser wakefield accelerator-based light sources," IOP, Plasma physics and Controlled Fusion, Vol. 58, Number 10, 2016

[6] J.C. Wood, D.J. Chapman, K. Poder, et al., "Ultrafast Imaging of Laser Driven Shock Waves using Betatron x-rays from a Laser Wakefield Accelerator," Scientific reports, Vol. 8, 11010, 2018

[7] Jason M. Cole, Daniel R. Symes, Nelson C. Lopes, et al., "High-resolution µCT of a mouse embryo using a compact laser-driven x-ray betatron source," PNAS, Vol. 115, Issue 25, pages 6335-6340, 2018

[8] A. E. Hussein, N. Senabulya, Y. Ma, "Laser-wakefield accelerators for high-resolution x-ray imaging of complex microstructures," Scientific reports, Vol. 9, page 1-13, 2019

[9] Instron, Universal Testing Systems, [Online]. Available: https://www.instron.com/en-us/products/testing-systems/universal-testing-systems

[10] Bruker, "object stages for In-Situ examination, 2022 [Online]. Available: https://www.bruker.com/content/bruker/int/en/products-and-solutions/microscopes/3d-x-ray-microscopes/object-stages-for-in-situ-examination.html

[11] Sherline, "Sherline products," 2022 [Online]. Available: https://www.sherline.com/

[12] Sparkfun Electronics, "OpenScale Applications and Hookup Guide," [Online]. Available: https://learn.sparkfun.com/tutorials/openscale-applications-and-hookup-guide.

[13] Node-RED, "node-red-dashboard," 7 July 2021. [Online]. Available: https://flows.nodered.org/node/node-red-dashboard

[14] pigpiod C Interface," 28 March 2021. [Online]. Available: https://abyz.me.uk/rpi/pigpio/pdif2.html

[15] S. Fourmaux, E. Hallin, U. Caulagain, S. Weber, and J. C. Kieffer, "Laser-based synchrotron x-ray radiation experimental scaling," Optical Society of America, Optics Express, Vol. 28, 3, pages 3147-3158, 2020

[16] V. Senthilkumaran, T. Richards, S. Knudsen, et al., "High-resolution betatron x-ray imaging of porosity evolution in additively manufactured alloys," 2021 IEEE International Conference on Plasma Science (ICOPS), 2021, page. 1-1

[17] J. A. Moore, S. F. Li, M. Rhee, and N. R. Barton, "Modeling the effects of grain and porosity structure on copper spall response," Springer, Journal of Dynamic Behaviour of Materials, Vol. 4, 4, pages 464-480, 2018

[18] M. Tang and P. C. Pistorius, "Anisotropic mechanical behavior of AlSi10Mg parts produced by selective laser melting," Springer, Jom, Vol. 69, 3, pages 516-522, 2017